International Journal of GEOMATE, May, 2025 Vol.28, Issue 129, pp.66-75
ISSN: 2186-2982 (P), 2186-2990 (O), Japan, DOI: https://doi.org/10.21660/2025.129.4865
Geotechnique, Construction Materials and Environment

SHEAR STRENGTH AND PERMEABILITY OF BENTONITE–CHITOSAN COMPOSITES WITH NATURALLY GRADED SANDS

Muhammad Salimi[1], *Yulian Firmana Arifin[1,2] , Muhammad Ansari[1]

[1]Faculty of Engineering, University of Lambung Mangkurat, Indonesia; [2]Wetland-Based Material Research Center, University of Lambung Mangkurat, Indonesia

*Corresponding Author, Received: 27 Dec. 2024, Revised: 11 Feb. 2025, Accepted: 12 Feb. 2025

ABSTRACT: The increasing need for sustainable materials in environmental engineering has driven research on eco-friendly clay liners. This study aimed to optimize the shear strength and permeability of chitosan–bentonite–sand composites by investigating the effects of sand grain distribution. Sands from various quarries with distinct gradations were used to explore composite performance under realistic conditions. Standard Proctor compaction determined the maximum dry density (1.64 g/cm³) and optimum moisture content. Direct shear tests (ASTM D3080) showed cohesion values of 9.77–18.64 kPa and internal friction angles of 26.37°–30.36°, demonstrating significant mechanical stability comparable to commercial clay liners. Characterization analyses (FTIR, XRD, SEM, and TGA) confirmed chitosan integration into the bentonite matrix, revealing chemical interactions, partial intercalation, morphological modifications enhancing cohesion, and improved thermal stability. Permeability values under standard compaction ranged from 5.7×10^{-8} cm/s to 6.9×10^{-8} cm/s, meeting regulatory limits. However, at 90% of MDD, permeability exceeded 1×10^{-7} cm/s for some samples, indicating sensitivity to compaction effort and grain distribution. Sands with well-graded distributions, particularly from Sungai Ulin and Barito River, exhibited higher shear strength, whereas those with poorer gradation had reduced internal friction angles. These results highlight the relationship between grain distribution and mechanical properties, emphasizing the need for optimized compaction to maintain both shear strength and permeability within acceptable limits.

Keywords: Bentonite, Chitosan, Permeability, Sand, Shear strength

1. INTRODUCTION

Composite materials that combine bentonite and sand are widely used in geotechnical and environmental engineering, particularly for landfill liners, hydraulic barriers, and waste containment systems. Bentonite, a clay mineral rich in montmorillonite, is highly valued for its low hydraulic conductivity and high swelling potential, which contribute to its effectiveness as an impermeable barrier. However, its swelling behavior can cause excessive pressure and shrinkage upon drying, potentially compromising structural integrity. To mitigate these challenges, sand is incorporated to balance mechanical stability and swelling properties, ensuring improved performance in applications requiring contaminant migration control [1–3].

Research has shown that the proportion of bentonite to sand is a critical factor in optimizing shear strength and compressibility, as different applications may prioritize sealing ability or structural robustness [4, 5]. For example, bentonite-rich mixtures enhance impermeability, whereas sand-rich composites improve stability under loading [6]. Additionally, bentonite particles fill the voids between sand grains, reducing permeability and enhancing contaminant containment, which is essential for waste management applications [3]. However, when bentonite content is low, particularly at 10%, permeability may exceed the regulatory threshold, making the composite unsuitable for liner applications. In such cases, additional materials, such as chitosan, are required to improve cohesion and reduce permeability [7].

With growing environmental concerns and the need for enhanced performance in low-bentonite mixtures, researchers have explored the use of sustainable organic additives to replace synthetic polymers in bentonite–sand composites. Trisoplast, a widely commercialized bentonite–sand–polymer composite, is a synthetic product with high shear strength and impermeability, cohesion values between 20 and 27.7 kPa, and internal friction angles (phi) ranging from 36.1° to 40.7° [8]. Despite its effectiveness, Trisoplast relies on non-biodegradable polymers, prompting interest in eco-friendly solutions. Chitosan, an organic biopolymer derived from chitin, has shown promise as an environmentally friendly alternative, providing improvements in the rheology, plasticity, and compressive strength of bentonite–sand mixtures [9]. Studies have shown that chitosan-amended soil can enhance consolidation characteristics and reduce shrinkage potential, making it a viable alternative for liner applications [10]. Additionally, the incorporation of chitosan has been found to improve erosion resistance and durability, further reinforcing its suitability as a stabilizing agent in geotechnical applications [11].

However, prior research has indicated that

chitosan–bentonite–sand composites still face limitations in terms of shear strength when compared to synthetic alternatives. Specifically, the shear strength of these composites remains lower than that of Trisoplast. For example, Salsabila et al. [12] reported that the maximum shear strength for chitosan–bentonite–sand composites yielded cohesion values of 7.79 and 9.11 kPa and internal friction angles of 26.68° and 23.03° under different compaction types, significantly lower than those of Trisoplast. Addressing this disparity requires a closer examination of the factors influencing the mechanical properties, such as sand particle distribution, which can play a critical role in enhancing the load-bearing capacity and overall stability of the composite.

Hidayat and Arifin [9] found that 2% chitosan optimizes permeability in clay liners, yet shear strength remains lower than commercial materials like Trisoplast. Erwansyah and Arifin [7] and Salsabila et al. [12] showed that a composite with 90% sand, 9.8% bentonite, and 0.2% chitosan met permeability standards ($1\times10^{-}7$ cm/s) but still had inferior shear strength. This highlights the need to optimize sand grain distribution to improve internal friction and structural performance.

Optimizing sand gradation may enhance the shear strength of these composites. Studies indicate that well-graded sand improves particle interlocking, increasing cohesion and internal friction, which are critical for load-bearing applications [13, 14]. This study aims to investigate the effects of varying sand gradations from different quarries on the shear strength of chitosan–bentonite–sand composites. While improved strength is expected, permeability remains a key consideration for regulatory compliance (1×10^{-7} cm/s). The novelty of this study lies in its focus on sustainable materials and the systematic evaluation of sand gradation for enhanced clay liner performance.

2. RESEARCH SIGNIFICANCE

This study advances eco-friendly geotechnical materials by optimizing chitosan–bentonite–sand composites for shear strength and permeability, which are essential for landfill liners and hydraulic barriers. By analyzing sands with varying grain distributions, it highlights the critical role of well-graded sand in enhancing internal friction angle, cohesion, and structural integrity. The inclusion of chitosan as a biodegradable alternative to synthetic polymers adds environmental benefits, meeting regulatory permeability requirements of 1×10^{-7} cm/s. This study bridges the gap between composite innovation and practical applications, advancing sustainable engineering while identifying areas for optimizing compaction and material composition.

3. MATERIALS AND METHODS

3.1 Bentonite

The Indonesian bentonite used in this study exhibits properties suitable for impermeable barriers and structural stability. With a specific gravity of 2.68, it aligns with industrial bentonites [15–18]. Its high liquid limit (310.49%) and plasticity index (259.45) indicate strong water absorption and flexibility, essential for containment applications [16, 19]. Classified as CH under the Unified Soil Classification System, it possesses high swelling capacity and compressibility [18, 20].

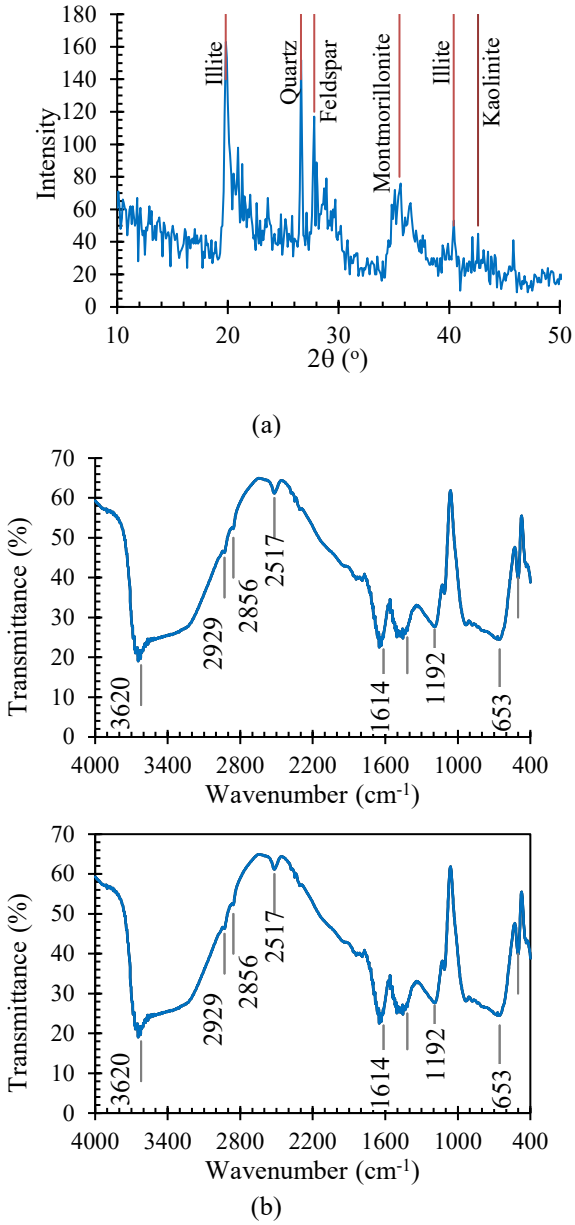

Fig. 1 (a) XRD pattern and (b) FTIR spectrum of bentonite used in this study

A cation exchange capacity (CEC) of 57 meq/100

g enhances its contaminant containment potential, comparable to widely used bentonites like MX80 [17] and GMZ01 [18]. XRD analysis confirms montmorillonite (35.51°), along with illite (19.81°, 40.41°), quartz (26.61°), feldspar (27.81°), and kaolinite (42.61°) (Fig. 1a), consistent with findings by Herbert et al. [21]. The absence of a low-angle peak likely results from instrumental limitations.

FTIR analysis (Fig. 1b) identifies montmorillonite's characteristic –OH stretching at 3620 cm^{-1}, Si–O stretching (1192 cm^{-1}), and Si–O–Al bending (653 cm^{-1}). Peaks at 2929 and 2856 cm^{-1} indicate organic impurities, while the 1614 cm^{-1} band corresponds to adsorbed water. Spectral comparisons with MX80 [17, 21], Kunigel [16], FEBEX [17], GMZ [18], and Kunibond bentonites reveal minor shifts due to compositional differences, with MX80 showing higher montmorillonite purity [21]. These findings highlight Indonesian bentonite's compatibility for composite applications with chitosan.

3.2 Chitosan

The chitosan used in this study is derived from crab and shrimp shells and prepared in powder form with a particle size range of 100–300 mesh. It has a degree of deacetylation of 87.5%, indicating a high level of purity and functional amine groups, which enhances its reactivity and suitability for applications in adsorption and composite formation.

3.3 Sand

The sand samples used in this study were collected from four locations: Barito River, Sungai Ulin, Landasan Ulin, and Palangkaraya. Additionally, one artificial sample was prepared by mixing sand from two locations, the Barito River and Sungai Ulin, in a 50:50 weight ratio. Fig. 2 illustrates the grain-size distribution curves for five sand samples, Barito River, Sungai Ulin, Landasan Ulin, Palangkaraya, and the artificial composite sample created by mixing the Barito River and Sungai Ulin sands. Based on the calculated coefficients of uniformity (Cu) and curvature (Cc), the samples from Barito River, Landasan Ulin, and Palangkaraya are classified as poorly graded sand (SP), whereas the Sungai Ulin and Barito River + Sungai Ulin samples are classified as well-graded sand-silty sand (SW-SM). These results highlight the variation in the particle size gradation among the samples, as reflected in the curves.

3.4 Composite Preparation

The preparation of the composite involved a standardized proportion of materials based on previous research findings: 0.2% chitosan, 9.8% bentonite, and 90% sand by weight. Chitosan and bentonite were mixed following the procedures suggested by Aguilar et al. [22] and Yang et al. [23] as adopted by Hidayat and Arifin (2023) to achieve an optimal ratio of 2% chitosan and 98% bentonite. The process began with the preparation of a 2% (v/v) acetic acid solution, into which 2 g of chitosan powder was added and stirred at 60 °C. Next, 98 g of bentonite was mixed with the chitosan solution and stirred for 2 h. Thereafter, the resulting mixture was combined with 100 mL of a 5.0% sodium tripolyphosphate solution and stirred for 4 h. Subsequently, the mixture was filtered, washed with distilled water until a neutral pH (pH 7) was achieved, and then dried in an oven at 60 °C until a fine powder was formed. This chitosan–bentonite mixture was then incorporated into the sand at a ratio of 0.2% chitosan, 9.8% bentonite, and 90% sand. Sand was gradually added while mixing to ensure uniform dispersion. The final composite mixture was homogenized using mechanical mixing techniques and shaped into molds for mechanical and permeability testing. The composite was further characterized by FTIR, XRD, TGA, and SEM to evaluate its chemical, structural, thermal, and microstructural properties, ensuring its suitability as an eco-friendly clay liner material.

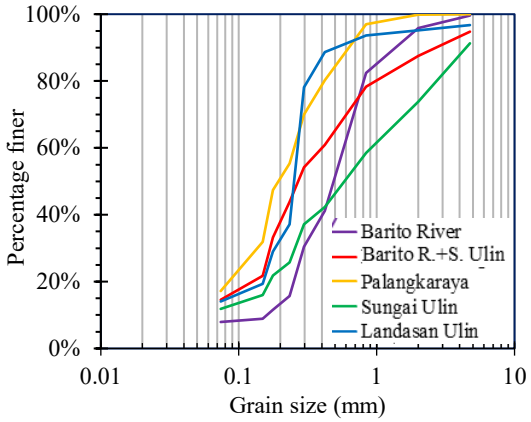

Fig. 2 Grain-size distribution of sand used in this study

3.5 Testing Procedures

The Standard Proctor Compaction Test (ASTM D698) was used to determine the maximum dry density and optimum moisture content of the chitosan–bentonite–sand composite. The samples were prepared and compacted according to these results, ensuring field-representative conditions based on the standard Proctor density. The Direct Shear Test (ASTM D3080) was used to assess shear strength and determine cohesion (c) and internal friction angle (φ) under simulated stress conditions. Permeability was evaluated using the falling head test to monitor water flow under a decreasing hydraulic head to measure hydraulic conductivity. These tests provided insights into the mechanical and hydraulic

performances of the composite, ensuring its suitability for containment applications.

4. RESULTS AND DISCUSSIONS

4.1 Characterization of Bentonite–Chitosan Composite

The FTIR spectra of bentonite, chitosan, and their composite reveal key functional groups, as illustrated in Fig. 3. Bentonite exhibits peaks at 505.35 cm^{-1}, 569 cm^{-1}, and 630.72 cm^{-1} (Si–O bending) and 1111 cm^{-1}, 1165 cm^{-1} (Si–O–Si stretching), with broad bands at 3261.63–3464.15 cm^{-1} linked to hydroxyl (-OH) stretching, consistent with previous reports [16, 24]. Chitosan shows absorption at 898.83–1269.16 cm^{-1} (C–O, C–H, amide) and broad bands at 2895.15–3078.39 cm^{-1} (O–H, N–H stretching), in agreement with Et-Tanteny et al. [25].

The bentonite-chitosan composite displays overlapping peaks from both materials, confirming their interaction. The peak at 2515.18 cm^{-1} suggests hydrogen bonding between chitosan's amino (-NH) and hydroxyl (-OH) groups with bentonite's silicate structure. Shifts in 3010.88–3209.55 cm^{-1} indicate further interfacial interactions, similar to findings by Bagheri et al. [26] and Ahari et al. [24].

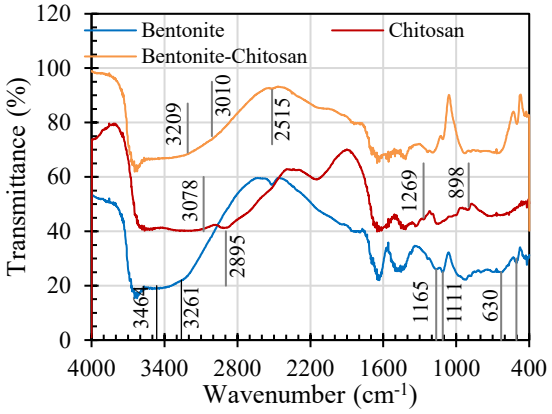

Fig. 3 FTIR spectra of bentonite, chitosan, and bentonite–chitosan composite

The presence of new peaks and slight shifts in the existing peaks of the composite suggest enhanced interactions between chitosan and bentonite, as noted by Yang et al. [23] and Bagheri et al. [26]. These interactions are critical for the structural stability and functionality of the composites.

The XRD patterns of bentonite and the bentonite–chitosan composite, as shown in Fig. 4, reveal structural modifications following chitosan intercalation. A noticeable decrease in peak intensity is observed for Illite (19.81°) and Montmorillonite (35.51°), while peaks corresponding to Feldspar (27.81°), Illite (40.41°), and Kaolinite (42.61°) disappear. These changes suggest alterations in the crystalline structure, likely due to interactions between bentonite layers and chitosan molecules.

Similar to Ahari et al. [24], a shift in bentonite peaks and reduced intensity suggest lattice distortion from molecular interactions between bentonite and chitosan. Additionally, a new peak appears at 28.51°, consistent with findings by Hidayat and Arifin [9], suggesting structural reorganization or new phase formation. These changes confirm the composite's altered crystallinity and potential new functional properties.

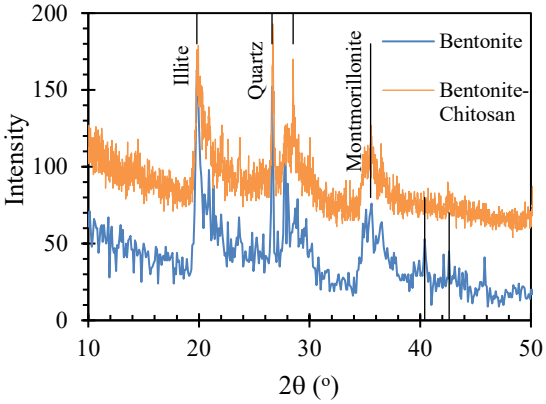

Fig. 4 XRD patterns of bentonite and bentonite–chitosan composite.

The TGA results for bentonite and the chitosan-bentonite composite revealed insights into their thermal stability and decomposition mechanisms. Fig. 5 presents the thermogravimetric analysis (TGA) curves for bentonite and the bentonite–chitosan composite, showing the percentage of mass retained (% TG) as a function of temperature.

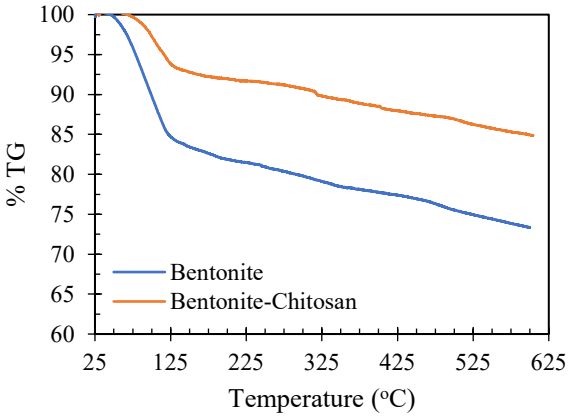

Fig. 5 Thermogravimetric analysis (TGA) curves of bentonite and chitosan–bentonite composite

Both materials exhibit a three-stage degradation process. The initial mass loss below 150°C is associated with the evaporation of hygroscopic and interlayer water. Bentonite shows a ~10% mass loss, whereas the composite retains more weight, losing only 5–7%. Between 150°C and 400°C, further mass loss occurs due to dehydroxylation and the thermal

degradation of chitosan, with bentonite experiencing a 15–20% reduction, while the composite exhibits a slower degradation rate of 10–12%. Beyond 500°C, the decomposition of bentonite's hydroxyl groups and the oxidation of residual chitosan carbon contribute to additional weight loss. At 600°C, bentonite retains 65–70% of its initial mass, whereas the composite retains 80–85%, indicating improved thermal stability due to chitosan integration.

The thermal degradation trends align with Ahari et al. **[24]**, showing similar mass loss stages for bentonite and bentonite–chitosan composites. Initial weight loss from water evaporation matches their findings (11.9% for bentonite, 28.36% for the composite). The slower mass loss between 150–400°C suggests enhanced thermal stability due to chitosan reinforcement, consistent with Rahman et al. [27] and Jeyaseelan et al. [28]. Above 500°C, greater mass retention in the composite supports findings by Ahari et al. **[24]** and Et-Tanteny et al. **[25]** on chitosan's stabilizing effect. Differential thermal analysis confirms an endothermic peak (~102°C) for water loss and exothermic peaks for chitosan decomposition, highlighting its role in thermal performance.

The SEM images at 1000× magnification provide an overview of the microstructural differences between pure bentonite (Fig. 6(a)) and the bentonite–chitosan composite (Fig. 6(b)). The bentonite sample exhibits a layered and flaky structure, characteristic of montmorillonite clay, with distinct plate-like morphology and relatively smooth surfaces. This structure reflects the typical aluminosilicate layers responsible for the adsorptive and ion-exchange properties of bentonite.

In contrast, the bentonite–chitosan composite presents a more aggregated and interconnected morphology, with visible coating-like formations on the bentonite surfaces. The presence of chitosan induces structural modifications, increasing particle agglomeration and forming a denser network. Similar morphological trends, where chitosan leads to an increase in cluster size, have been reported by Hidayat and Arifin [9], reinforcing the role of polymer addition in altering bentonite's surface characteristics.

At 20,000× magnification, SEM analysis of pure bentonite (Fig. 7(a)) and the chitosan–bentonit composite (Fig. 7(b)) reveals significant morphological differences, indicating chitosan integration. Pure bentonite exhibits a layered, flaky structure with a relatively smooth, plate-like morphology, characteristic of montmorillonite clay and its aluminosilicate layers, which contribute to adsorptive and ion-exchange properties. The chitosan–bentonit composite, however, displays a rougher, more irregular surface with additional aggregates and coating-like structures (Fig. 7(b)). These modifications suggest successful chitosan adhesion, altering the surface texture and forming a denser, more interconnected morphology. This transformation likely results from interactions between chitosan's hydroxyl and amine groups and the bentonite surface, including interlayer regions.

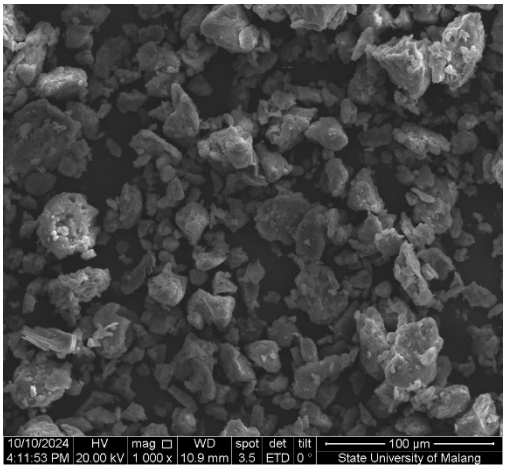

(a)

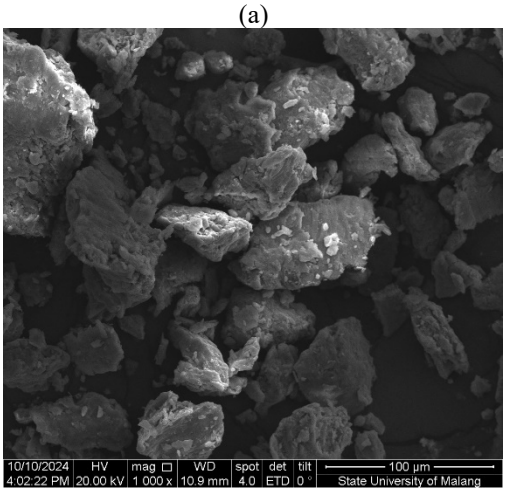

(b)

Fig. 6 SEM micrographs of pure bentonite (a) and chitosan–bentonite composite (b) at 1000×

4.2 Compaction Test Results

The compaction behavior of the bentonite–chitosan-sand mixture sourced from Sungai Ulin was evaluated under two compaction conditions, revealing distinct density and moisture relationships. As shown in Fig. 8, the maximum dry density (MDD) reached 1.655 g/cm³ for Compaction 1 and 1.640 9/cm³ for Compaction 2, both occurring at an optimum moisture content (OMC) of approximately 11.5%. These results highlight the material's response to compaction energy and its potential for achieving adequate field density.

To establish a reference value for the density, the MDDs from the two conditions were averaged, yielding an MDD of 1.648 g/cm³. The average value was used as the standard compaction density for subsequent analyses. The consistent OMC and

similar MDD values highlight the uniform compaction behavior of the chitosan–bentonite–sand mixture, emphasizing the suitability of Sungai Ulin sand for maintaining stable density and moisture characteristics during compaction.

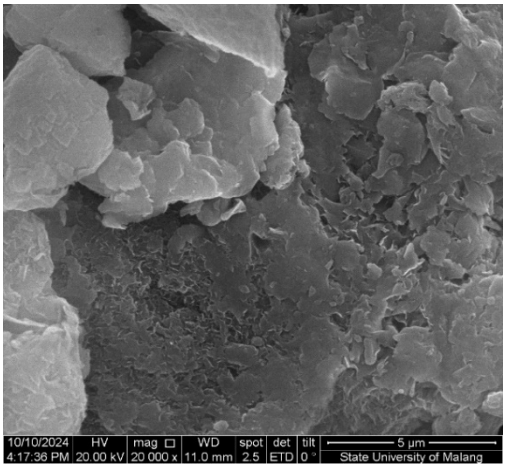

(a)

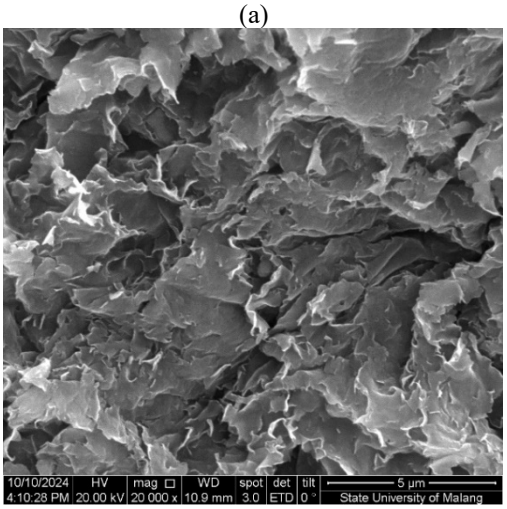

(b)

Fig. 7 SEM micrographs of pure bentonite (a) and chitosan –bentonite composite (b) at 20000×.

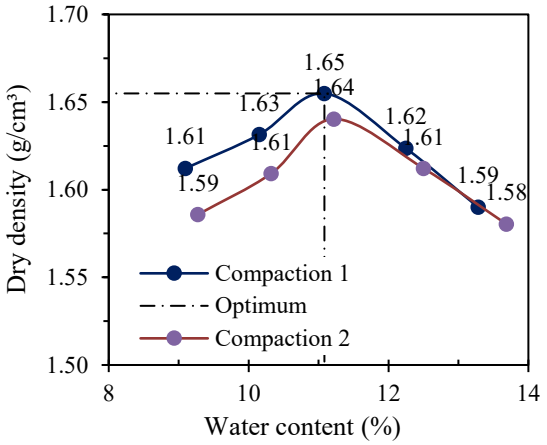

Fig. 8 Compaction test result of chitosan–bentonite–sand mixture

4.3 Shear Strength Analysis

Table 1 and Fig. 9 present critical insights into the mechanical behavior of the chitosan–bentonite–sand composite, focusing on its shear strength properties. The table provides cohesion (c) and internal friction angle (ϕ\phi) values for different sand sources, comparing pure sand and bentonite-chitosan-sand mixtures. Cohesion values range from 9.77 kPa for the Palangkaraya sand to 18.64 kPa for the Sungai Ulin sand, reflecting variations in bonding strength due to chitosan's addition. The internal friction angles also show enhancement with chitosan, with significant increases in Sungai Ulin sand from 30.36° to 33.54°. These findings are consistent with those of Ahari et al. [25], who demonstrated the ability of chitosan to improve the mechanical properties of composites by modifying the interparticle bonding and structure. Similarly, Daheur et al. [29] explored mixtures of local materials, such as tuff and sand, emphasizing the role of matrix stabilization in mechanical enhancements.

Table 1. Cohesion (c) and internal friction angle (ϕ) of chitosan–bentonite–sand mixtures based on sand source

Source of sand	Bentonite–chitosan–sand		Sand
	c (kPa)	ϕ (°)	ϕ (°)
Barito River	14.82	26.37	28.96
Sungai Ulin	18.64	30.36	33.54
Barito R.+ Sungai Ulin	11.99	28.4	31.58
Landasan Ulin	13.8	28.4	29.19
Palangkaraya	9.77	26.38	31.58

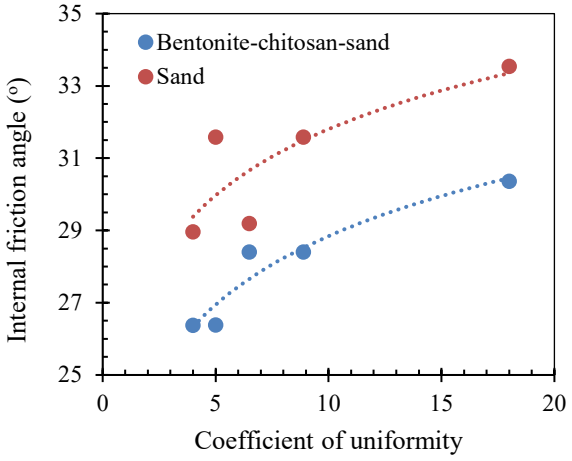

Fig. 9 Relationship between Cu and ϕ for sand and chitosan–bentonite–sand mixtures.

The relationship between internal friction angles and grain uniformity was analyzed for both pure sand and chitosan– bentonite–sand composites, revealing distinct trends. As shown in Fig. 9, the composite

consistently exhibits lower internal friction angles than pure sand, primarily due to the cohesive nature of chitosan, which reduces the frictional contribution of angular sand particles. However, both materials display a similar increasing trend with higher coefficients of uniformity (Cu), indicating that improved grain distribution enhances shear resistance despite the presence of cohesion in the composite.

The shear strength results of the chitosan–bentonite–sand composite in this study ranged from 9.77 kPa to 18.64 kPa for cohesion (c) and 26.37° to 30.36° for the internal friction angle (ϕ), slightly higher than those reported by Salsabila et al. [12]. The limited increase in cohesion is due to the similar bentonite and chitosan content, which primarily contribute to cohesion. The key difference lies in the sand used—Salsabila et al [12]. utilized poorly graded sand, while this study used sands with varying grain distributions. The results show that a higher coefficient of uniformity (Cu) leads to an increased internal friction angle. Similar trends were observed by Erwansyah and Arifin [7], where cohesion increased with higher bentonite content, while friction angles decreased due to the material's cohesive nature. Compared to Trisoplast [29], which exhibited friction angles of 36.1°–40.7° at a higher density (1.76–1.82 g/cm³), the sand in this study achieved comparable friction angles despite a lower density of 1.64 g/cm³, highlighting its contribution to shear resistance.

The FTIR, XRD, TGA, and SEM analyses collectively provide insights into the shear strength and compaction behavior of the chitosan–bentonite–sand composites. FTIR spectroscopy confirms successful chemical bonding between chitosan and bentonite, with characteristic peak shifts indicating enhanced cohesion and reduced desiccation cracking. XRD reveals structural changes, such as increased d-spacing and reduced crystallinity, improving flexibility and stability while boosting the cohesive strength in direct shear tests.

TGA highlights the enhanced thermal stability with slower degradation rates than pure bentonite, reflecting the stabilizing effects of chitosan and the protective framework of bentonite. These results align with those of previous studies, such as that of Ahari et al. [24], demonstrating the reinforcing role of biopolymers in clay materials. The SEM micrographs further validate these findings, showing denser and rougher surfaces in the composite, indicating successful chitosan integration and improved mechanical interlocking for better shear resistance.

4.4 Permeability of Chitosan–Bentonite–Sand Composite

The permeability values, derived from two compaction conditions, i.e., 1.64 g/cm³ (MDD) and 90% of MDD, reveal critical insights into the performance of the chitosan–bentonite–sand composite (Table 2). A 90% MDD is typically the minimum field compaction requirement that must be satisfied during the compaction process to ensure adequate soil performance. For clay liners, a permeability criterion of 1×10^{-7} cm/s is a commonly accepted standard in many countries worldwide.

Table 2. Permeability values of compacted chitosan–bentonite–sand samples

Source of sand	k_1 (cm/s)	k_2 (cm/s)
Barito River	5.70E-8	2.57E-07
Sungai Ulin	6.97E-8	8.77E-07
Barito R.+ Sungai Ulin	5.79E-8	8.90E-07
Landasan Ulin	5.92E-8	1.09E-07
Palangkaraya	6.86E-8	7.53E-8

k_1: Permeability at MDD; k_2: Permeability at 90% MDD

Under standard Proctor compaction at a density of 1.64 g/cm³, the permeability values range from 5.7 x 10^{-8} cm/s to 6.9 x 10^{-8} cm/s, all of which meet the regulatory requirements. However, these values are uncomfortably close to the allowable limit, indicating high sensitivity to variations in compaction effort, moisture content, or material composition, particularly for sands from Sungai Ulin and Palangkaraya, which exhibit the highest permeability within this range. Interestingly, at 90% MDD, samples with the best shear strength performance and favorable coefficient of uniformity (Cu), such as those from Sungai Ulin and Barito River, fail to maintain permeability within acceptable limits. This divergence between shear strength and permeability performance highlights the trade-offs inherent in designing chitosan–bentonite–sand composites. Although the material performs well mechanically under these compaction conditions, its hydraulic behavior requires careful management to ensure compliance with clay liner standards.

To address this challenge, further research is required to evaluate the performance of these composites using modified Proctor compaction techniques. Enhanced compaction methods may help achieve lower permeability while maintaining or improving shear strength, enabling the material to meet the stringent regulatory requirements for clay liners and other geotechnical applications.

The relationship between permeability coefficients and dry density was analyzed across various materials and studies, including those from this research, commercial clay liners, and other referenced composites. As shown in Fig. 10, the dashed horizontal line marks the permeability

threshold of 1×10^{-7} cm/s, widely recognized as the standard for clay liners. Most data points fall below this limit, confirming that the tested materials generally meet regulatory requirements.

The permeability values in this study (highlighted in red) align closely with the regulatory limit at densities near 1.64 g/cm³, demonstrating that the chitosan–bentonite–sand composite meets the standard for clay liners. While proximity to the limit suggests scope for improvement, it does not indicate failure, but rather highlights the potential for refinement. The success of this material lies in its ability to balance permeability with shear strength and environmental sustainability, making it a promising alternative to traditional materials.

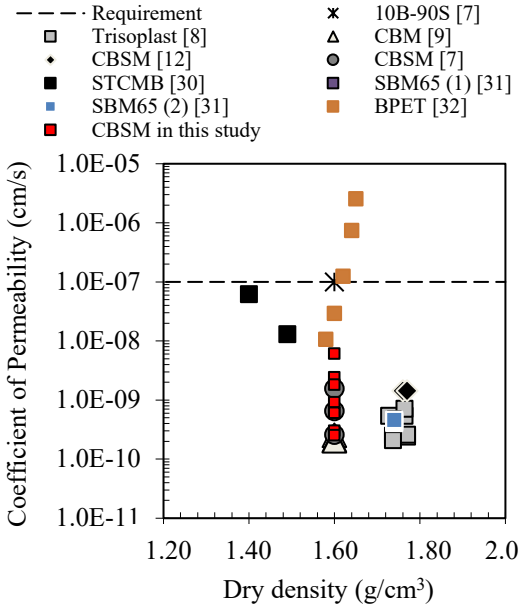

Fig. 10 Coefficient of permeability as a function of dry density of various polymer–bentonite composites.

The STCMB, represented by black squares, consists of sand with bentonite modified with tetramethylammonium bromide and sodium carboxymethylcellulose [30]. This composite exhibits lower permeability values, reflecting the effectiveness of chemical modification and polymer addition in enhancing its hydraulic performance. Similarly, SBM65, which combines pure bentonite with 65% sand content and polymers such as Xanthan gum and Guar gum, demonstrates excellent performance with lower permeability values, as indicated by the blue markers [31]. BPET, another high-performance composite (green squares), combines bentonite with environmentally friendly polymers, further reinforcing the versatility of polymer-enhanced materials [32].

CB, depicted by a triangle, is a mixture of 90% chitosan and 10% bentonite [9]. CBS, represented by diamonds, is a chitosan–bentonite–sand mixture comprising 70%–90% sand [7], 90% sand, 9.8% bentonite, and 0.2% chitosan [12]. Its permeability values are similar to those in this study, reinforcing the efficacy of chitosan as a stabilizing agent in such mixtures. Trisoplast, a widely used commercial material for clay liners (white squares), demonstrates superior permeability [8]. Its well-established application underscores its reliability under field conditions, and the materials used in this study present a more sustainable and cost-effective approach.

The comparison highlights that the chitosan–bentonite–sand mixture developed in this study is competitive and meets the essential requirements of clay liners. Future optimization, particularly through refined compaction techniques and tailored material compositions, can further enhance its performance. These findings validate the approach adopted in this study and demonstrate its success and contribution to advancing eco-friendly geotechnical applications. Similar studies on marine clay [33] and polyurethane-clay mixtures [34] have also explored alternative materials for landfill liners, highlighting the importance of optimizing material composition and compaction methods to achieve desirable mechanical and hydraulic properties.

5. CONCLUSION

This study successfully investigated the optimization of shear strength in bentonite–chitosan–sand composites by analyzing the effects of sand grain distribution on the mechanical and hydraulic properties. The results demonstrated that the shear strength of the composite, characterized by the cohesion and internal friction angle, can be effectively enhanced by controlling the gradation of sand. Sands with well-graded distributions, particularly those sourced from Sungai Ulin and Barito River, exhibited improved internal friction angles, though the permeability values approached the regulatory limit of 1×10^{-7} cm/s, highlighting the sensitivity of the material to compaction and moisture variations.

Permeability measurements further indicate that the composite meets the permeability requirements for clay liners but remains close to the threshold, particularly under Standard Proctor compaction conditions. This study highlights the importance of achieving optimal compaction and material proportions, suggesting that future work should explore Modified Proctor compaction methods to further enhance performance.

6. ACKNOWLEDGMENT

This research was supported by the DRTPM Grant Program under contract numbers 056/E5/PG.02.00. PL/2024 and 1013/UN8.2/PG/2024, funded by the

Indonesian Ministry of Higher Education, Science, and Technology.

7. ABBREVIATIONS

ASTM	American society for testing and materials
FTIR	Fourier–transform infrared spectroscopy
SEM	scanning electron microscopy
XRD	X-ray diffraction
TGA	thermogravimetric analysis
LL	liquid limit
PI	plasticity index
CEC	cation exchange capacity
FEBEX	full–scale engineered barrier experiment
GMZ	Gaomiaozi (a type of bentonite from China)
MX80	a bentonite from Wyoming, USA
Cu	coefficient of uniformity
Cc	coefficient of curvature
CH	clay-high plasticity
SP	poorly graded sand
SW	well–graded sand
SM	silty sand
OMC	optimum moisture content
MDD	maximum dry density
CB	chitosan–bentonite
CBS	chitosan–bentonite–sand
STCMB	tetramethylammonium–carboxymethyl cellulose–modified bentonite sand
SBM	sand–bentonite mixture
BPET	bentonite–polymer enhanced treatment

8. REFERENCES

[1] Alzamel M., Fall M. Effect of Pore Water Salinity on Swelling Hehavior, and Mineralogical and Microstructural Properties of Bentonite-Sand Barrier Materials. Proceedings of the 3rd International Conference of Recent Trends in Environmental Science and Engineering (RTESE'19), 2019, pp. 1–4.

[2] Srikanth V., Mishra A.K. A Laboratory Study on the Geotechnical Characteristics of Sand–Bentonite Mixtures and the Role of Particle Size of Sand. International Journal of Geosynthetics and Ground Engineering, Vol. 2, Issue 1, 2016, pp. 1–10.

[3] Barrima A., Mashhour I.M., Amer N.H. Effect of Bentonite Content on Hydraulic Conductivity of Sand-Bentonite Mixtures Used in Landfill Liners as an Alternative to Clay Liner in Egypt. IOP Conference Series: Earth and Environmental Science, Vol. 1056, Issue 1, 2022.

[4] Güneri E., Yükselen Aksoy Y. Shear strength behaviour of sand-bentonite mixtures with pumice additivite under high temperature. E3S Web of Conferences, Vol. 205, 2020, pp. 4–6.

[5] Zeng Z., Cui Y.-J., Talandier J. Investigating the swelling pressure of highly compacted bentonite/sand mixtures under constant-volume conditions. Acta Geotechnica, Vol. 17, 2021.

[6] Kohno M., Nara Y., Kato M., Nishimura T. Effects of clay-mineral type and content on the hydraulic conductivity of bentonite–sand mixtures made of Kunigel bentonite from Japan. Clay Minerals, Vol. 53, Issue 4, 2018, pp. 721–732.

[7] Erwansyah E., Arifin Y.F. Chitosan-enhanced bentonite-sand mixture as a clay liner. AIP Conference Proceedings, Vol. 3110, Issue 020032, 2024, pp. 1–6.

[8] Schanz T., Agus S.S., Tscheschlok G. Hydraulisch-mechanische Eigenschaften einer polymerverbesserten Sand-Bentonit-Mischung beim Einsatz im Deponiebau. Geotechnik, Vol. 27, Issue 4, 2004, pp. 344–355.

[9] Hidayat T., Arifin Y.F. The Potential of Bentonite and Chitosan Mixtures as Clay Liner Base Material. IOP Conference Series: Earth and Environmental Science, Vol. 1184, 2023, pp. 1–8.

[10] Rasheed R.M., Moghal A.A.B., Jannepally S.S.R., Rehman A.U., Chittoori B.C.S. Shrinkage and Consolidation Characteristics of Chitosan-Amended Soft Soil—A Sustainable Alternate Landfill Liner Material. Buildings, Vol. 13, Issue 9, 2023.

[11] Rasheed R.M., Moghal A.A.B., Rambabu S., Almajed A. Sustainable assessment and carbon footprint analysis of polysaccharide biopolymer-amended soft soil as an alternate material to canal lining. Frontiers in Environmental Science, Vol. 11, Issue June, 2023, pp. 1–14.

[12] Salsabila N., Arifin Y., Pratiwi A. Compaction Parameters of a Chitosan-Bentonite-Sand Mixture., in Rahim, R., Suhartono, E. (Eds.): 'The 1st International Conference on Environmental Science, Development, and Management, ICESDM' (EAI, 2024), pp. 1–8.

[13] Babatunde Q.O., Kim H.J., Byun Y.H. Enhancing shear strength of sandy soil using zein biopolymer. Results in Engineering, Vol. 24, Issue September, 2024, p. 102891.

[14] Othman B.A., Marto A., Pakir F., Salikin A. Influence of Grain Sizes on Undrained Strength of Sand Mixtures. International Journal of Innovative Technology and Exploring Engineering, Vol. 8, Issue 9, 2019, pp. 3154–3159.

[15] Schanz T., Arifin Y.F., Khan M.I., Agus S.S. Time effects on total suction of bentonites. Soils and Foundations, Vol. 50, Issue 2, 2010, pp. 195–202.

[16] Sun Z., Chen Y.G., Ye W.M., Wang Q., Wu D.B., Yin Z.Y. Effects of synthetic site water

on bentonite-concrete system for a potential nuclear waste repository. Journal of Rock Mechanics and Geotechnical Engineering, Vol. 16, Issue 9, 2024, pp. 3786–3797.

[17] Lu Y., McCartney J.S. Free swelling behavior of MX80 bentonite under elevated temperatures up to 200 °C. Geomechanics for Energy and the Environment, Vol. 37, 2024.

[18] Ruan K., Komine H., Wang H., Ito D., Gotoh T. Experimental study on swelling pressure of low dry density compacted bentonites during saturation combining X-ray diffraction. Canadian Geotechnical Journal, Vol. 60, Issue 4, 2023, pp. 566–579.

[19] Liu Y.M. Influence of heating and water-exposure on liquid limit of GMZ01 and MX80 bentonite., in 'Unsaturated Soils: Theoretical and Numerical Advances in Unsaturated Soil Mechanics - Proceedings of the 4th Asia Pacific Conference on Unsaturated Soils' (2010), pp. 149–152.

[20] Sudheer Kumar R., Warr L.N., Grathoff G.H., Thombare B.R. Advanced smectite alteration and the role of accessory reactants at 180 °C: New experimental constraints on the stability of bentonite. Applied Clay Science, Vol. 260, 2024.

[21] Herbert H.J., Kasbohm J., Nguyen-Thanh L., et al. Alteration of expandable clays by reaction with iron while being percolated by high brine solutions. Applied Clay Science, Vol. 121–122, 2016, pp. 174–187.

[22] Aguilar R., Nakamatsu J., Ramírez E., et al. The potential use of chitosan as a biopolymer additive for enhanced mechanical properties and water resistance of earthen construction. Construction and Building Materials, Vol. 114, 2016, pp. 625–637.

[23] Yang Y., Xu Y., Zhong D., Qiao Q., Zeng H. Efficient removal of Cr(VI) by chitosan cross-linked bentonite loaded nano-zero-valent iron composite: Performance and mechanism. Journal of hazardous materials, Vol. 480, 2024, p. 136183.

[24] Ahari M., Hadoudi N., Zaki N., et al. Adsorption of bisphenol A (BPA) and pentachlorophenol (PCP) using a bentonite-chitosan composite: A study on removal efficiency. Inorganic Chemistry Communications, Vol. 165, Issue April, 2024, p. 112468.

[25] Et-tanteny R., Amrani B. El, Benhamou M. Investigation and modeling of physicochemical properties of bentonite-chitosan composites versus the concentration of chitosan added by intercalation. Chemical Physics Impact, Vol. 8, Issue June, 2024, p. 100611.

[26] Bagheri K., Kaviani A., Pircheraghi G., Shahidizadeh A. Dispersion-promoted synergistic cationic dye removal through the co-introduction of natural diatomite and bentonite into chitosan-based hydrogel beads. Sustainable Materials and Technologies, Vol. 42, 2024, p. e01166.

[27] Rahman M., Maniruzzaman M., Gafur M., et al. Fabrication of chitosan coated bentonite clay multifunctional nanosorbents from waste biomass for the effective elimination of hazardous pollutants from waterbodies: A fixed bed biosorption, mechanism, and mathematical model study. International Journal of Biological Macromolecules, Vol. 282, 2024, p. 137439.

[28] Jeyaseelan A., Natrayasamy V., Naushad M. Design and development of rare earth elements anchored pectin/chitosan integrated magnesia hybrid composite for effective defluoridation of water. Separation and Purification Technology, Vol. 352, 2024, p. 128137.

[29] Daheur E.G., Taibi S., Goual I., Li Z. Sen Hydro-mechanical behavior from small strain to failure of tuffs amended with dune sand – Application to pavements design in Saharan areas. Construction and Building Materials, Vol. 272, 2021, p. 121948.

[30] Ni H., Fan R.D., Reddy K.R., Du Y.J. Containment of phenol-impacted groundwater by vertical cutoff wall with backfill consisting of sand and bentonite modified with hydrophobic and hydrophilic polymers. Journal of Hazardous Materials, Vol. 461, Issue September 2023, 2024, p. 132627.

[31] Biju M.S., Arnepalli D.N. Effect of biopolymers on permeability of sand-bentonite mixtures. Journal of Rock Mechanics and Geotechnical Engineering, Vol. 12, Issue 5, 2020, pp. 1093–1102.

[32] Chandra A., Siddiqua S. Sustainable utilization of chemically depolymerized polyethylene terephthalate (PET) waste to enhance sand-bentonite clay liners. Waste Management, Vol. 166, 2023, pp. 346–359.

[33] Zarime N. 'Aishah, Solemon B., Yaacob W.Z.W., Wahab W.A., Omar R.C., Isa A.A.M. the Potential of Marine Clay Used for Landfill Liner: a Geotechnical Study. International Journal of GEOMATE, Vol. 25, Issue 107, 2023, pp. 228–234.

[34] Frianeza C.D., Adajar M.A.Q. Lateral Shrinkage of Compacted Polyurethane-Clay Subjected To a Single Wet-Dry Cycle. International Journal of GEOMATE, Vol. 26, Issue 115, 2024, pp. 1–8.